ACS APPLIED MATERIALS & INTERFACES

Functional Inorganic Materials and Devices

Self-Powered Motion-Driven Triboelectric Electroluminescence Textile

Hye-Jeong Park, SeongMin Kim, Jeong Hwan Lee, Hyoung Taek Kim, Wanchul Seung, Youngin Son, Tae Yun Kim, Usman Khan, Nae-Man Park, and Sang-Woo Kim

ACS Appl. Mater. Interfaces, **Just Accepted Manuscript** • DOI: 10.1021/acsami.8b16023 • Publication Date (Web): 04 Jan 2019

Just Accepted

ACS Publications

is published by the American Chemical Society. 1155 Sixteenth Street N.W., Washington, DC 20036

Self-Powered Motion-Driven Triboelectric Electroluminescence Textile

Hye-Jeong Park[1,⊥], SeongMin Kim[1,⊥], Jeong Hwan Lee[1], Hyoung Taek Kim[1], Wanchul Seung[1], Youngin Son[1], Tae Yun Kim[1], Usman Khan[1], Nae-Man Park[2], and Sang-Woo Kim[1] *

[1]School of Advanced Materials Science and Engineering, Sungkyunkwan University (SKKU), Suwon 16419, Republic of Korea, [2]Electronics and Telecommunications Research Institute (ETRI), Daejeon 34129, Republic of Korea

Corresponding Author *E-mail: kimsw1@skku.edu (S.-W. Kim)

ABSTRACT

In recent years, smart light emitting type electronic devices for wearable applications have been required to have flexibility and miniaturization, which limits the use of conventional bulk batteries. Therefore, it is important to develop a self-powered light emitting system. Our study demonstrates the potential of a new self-powered luminescent textile system that emits light driven by random motions. The device is a ZnS:Cu based textile motion-driven electroluminescent device (TDEL) fabricated onto the woven fibers of the ZnS:Cu embedded PDMS (Polydimethylsiloxane) composite. Triboelectrification, which raises a discontinuous electric field, is generated by the contact separation movement of the friction material. Therefore, light can be generated via triboelectrification by the mechanical deformation of the ZnS:Cu embedded PDMS composite. This study showed that the TDEL emitted light from the internal triboelectric field during contact and from the external triboelectric field during separation. Light was then emitted twice in a cycle, suggesting that continuous light can be emitted by various movements, which is a key step in developing self-powered systems for wearable applications. Therefore, this technology is a textile motion-driven electroluminescence system based on composite fibers (ZnS:Cu + PDMS) and PTFE fibers, and the proposed self-emitting textile system can be easily fabricated and applied to smart clothes.

KEYWORDS: *triboelectrification; electroluminescence; luminescent textile; motion-driven; woven structure*

INTRODUCTION

Mechanoluminescence is the emission of the radiation from a material that is caused by external stimuli such as strain or force. For example, direct mechanical stress on an object induces piezo- or fracto-luminescence from it; meanwhile, the application of mechanical stress on the embedded phosphor particles in a matrix can also induce piezo- or tribo-luminescence indirectly.[1–4] Furthermore, photoabsorption[5,6], electric fields[7–9], and chemical reactions[10,11] can also induce luminescence. As an electric field type, triboelectric charges that are generated by electron transfers due to the effective work function difference between two triboelectric materials, after the equilibrium state of Fermi level has been reached, can potentially modify the surrounding electric potential.[12–14] Because of the change in the electric potential, the underlying phosphor particles inside a matrix can then be excited to reach luminescence. These various types of stimuli can be used to cover a wide range of practical applications.[15–18]

Among the various applications, luminescent textiles are gaining importance regarding health care and personal safety wearable electronic devices.[19–24] In particular, the night time alerting of users of the presence of other people in their vicinity could be crucial in the enhancement of public safety. However, during the manufacturing of flexible electronic systems, the luminescence textiles face technological challenges regarding flexibility and robustness. In addition, numerous technical problems still need to be solved for the miniaturization of the control electronics and the battery and to minimize the number of interconnections. One possible solution to this challenge is the self-powering of the textile systems that have been combined with the luminescence without the use of bulky and limited lifetime batteries.[25–30] Here, a novel textile motion-driven electroluminescence (TMEL) system that does not comprise a battery and interconnection lines is presented. It is actually a triboelectrification-driven electroluminescence system, where the mechanical interactions

between the textile fibers produce a radiation emission due to a stretching motion. It should be noted that the triboelectrification-driven electroluminescence is thoroughly different from the well-known triboluminescence that light is generated through the breaking.

RESULTS AND DISCUSSION

In this work, a woven-structured composite material is constructed in order to investigate the double triboelectrification-induced electroluminescence (TI-EL: internal + external effects). The fabric structure consists of the following two parts: (i) a luminescent part and (ii) polytetrafluoroethylene (PTFE), as shown in Figure 1a. Figure 1b shows a cross-sectional field emission-scanning electron microscopy (FE-SEM) image of a luminescent region, indicating the average diameter of the zinc sulfide (ZnS):copper (Cu) particles that is approximately 30 μm (the dashed lines indicate the border lines of the luminescent region). The details of the TMEL fabrication process that consists of the ZnS:Cu and polydimethylsiloxane (PDMS) composites are illustrated in Figure S1. Figure S2 demonstrates that the plain woven textile structure can be easily stretched diagonally, while it provides a continuous surface friction between the warp and the weft. Besides, the plain structure is the simplest woven pattern that can provide the highest durability in various directions.

To compare the luminescent intensity between the two different fabric structures, one of the woven structures, which is shown in Figure 1c, consists of only the luminescent material of the ZnS:Cu with the PDMS, and the other structure, which is shown in Figure 1e, consists of the weft (luminescent material) and the wart (PTFE). The same displacement change (~ 3 cm) was produced by stretching both of the structures along the x-axis, as shown in Figure 1c and 1e. Figure 1d and 1f show the luminescence intensity distribution as a function of the wavelength for each case. When a separate luminescent weft rubs against the triboelectrification warp,

instantaneous light emits from the entirety of the woven structures, as shown in Figure 1c and 1e. Major peaks occurred at 518 nm for both cases. However, the one consisting of two materials (the luminescent material for the weft and the triboelectric material for the warp) clearly shows a greater intensity.

For understanding the luminescence mechanism and the quantification of the difference in the luminescence intensities that is due to the different friction materials, the friction objects shifted in the vertical direction, while the light emission was simultaneously monitored, as shown in Figure 2a and S3. The PTFE, poly(4,4'-oxydiphenylene-pyromellitimide) (Kapton), and the PDMS were utilized as the triboelectric layers for the comparison. A pressure sensor was installed at the top of the moving object and displayed at the bottom of the equipment to check and control the contact pressure at the frictional interface. The luminescence measurement process is as follows. A square object (1 x 1 cm^2) that is covered by the friction material (triboelectrification layer) is moved down to make contact with the luminescent layer of the ZnS:Cu with the PDMS composite at a frequency of 5 Hz, while a spectrometer-connected optical-fiber probe with a focusing lens (the probe and the lens are approximately 1 cm apart) is positioned in the dark acryl box close to the back of the luminescent layer to measure the luminescence. This is how the emitted light is guided to the spectrometer during the contact and the separation. Additionally, the luminescence was also measured when the sample was compressed by the vertical pushing force.

It is suggested that the luminescence of the ZnS:Cu phosphor particles in these complex systems can be excited by two ways including those where the internal and external electric fields are use.[15–17] To separate these two effects to understand the luminescence mechanism, two controlled experiments were prepared wherein the pushing states were manipulated to measure the luminescence intensity. As is schematically presented in Figure 2b and S4, it was

firstly assumed that the pores around the phosphors can locally induce the electric field for the internal triboelectrification-induced EL case.[17,31] Secondly, for the external triboelectrification-induced EL case, the electric field from the external interface can generate the luminescence in the phosphors. It is well known that the frictional contact between two triboelectric materials can generate triboelectrification charges with opposite signs at the contact interfaces. The triboelectrification charges can change the surrounding electric potential, thereby exciting the EL in the embedded phosphor particles.

To clarify the two factors that can influence the luminescence, the luminescence intensity was directly measured in two categories under the contact–separation mode of the triboelectric nanogenerator (TENG). As shown in Figures 2c and 2d, one cycle during 200 ms consists of double luminescence-intensity peaks with different peak ratios for the PTFE, but almost the same ratio is evident for the Kapton under the compressive load of 3 kgf. The first peak indicates that the intensity is due to the internal triboelectrification-induced luminescence during the contact where the pore interfaces between the ZnS:Cu particle and the PDMS are formed due to the elastic PDMS. The second peak indicates that the intensity is from the external triboelectrification-induced luminescence after the contact where the charged interface between the PDMS and the PTFE (or the Kapton) changes the electric potential of the ZnS:Cu phosphors. Regardless of the triboelectrification layer (the PTFE or PDMS), the intensity of the internal triboelectrification-induced EL is measured as similar for the two cases, but a slight force increase is evident because the pore sizes might also increase with the increasing of the force, as shown in Figure 2f. The peak ratios of the second to the first are 3.1 and 1.2 for the PTFE and the Kapton, respectively. Figure 2e shows the luminescent intensity as a function of the force for the external triboelectrification-induced EL, and the force dependence is greater than that for the internal triboelectrification-induced EL, as shown in Figure 2f. In Figure S5,

the luminescence varies with the different forces, but the peak PTFE and Kapton positions are the same at the 510 nm wavelength (green color).

Figure 3a shows the compression system which consists of a metallic material that was applied to the SEM holder to induce deformation to the ZnS:Cu-PDMS composite film in the vertical direction. In the initial state without the external force, the pores are naturally formed at the interface between ZnS:Cu phosphor and PDMS; the weak adhesion of ZnS:Cu and PDMS allows air to enter at the interface, as shown in Figure S6. When the external force was applied to this film, as shown in Figure 3b, it decreased to around 85 % of the original thickness and the pores formed to the right- and left-side of ZnS:Cu phosphor inside the PDMS matrix. The increased pores around ZnS:Cu phosphor recovered without deformation by the external force in Figure 3c.

The small size pores that are formed inside the PDMS matrix could produce a relatively small triboelectrification, where the PDMS is negatively changed relative to the ZnS, compared with that from the larger contact area of the external triboelectrification.[12,32,33] In addition, the luminescence intensity that is due to the PTFE contact that is greater than that from the Kapton contact can be explained in terms of the triboelectric series. In fact, the PTFE and the Kapton are relatively negative and positive compared with the PDMS, respectively.[12] Since the luminescence is closely associated with the triboelectrification, the output voltage that is generated due to the triboelectrification can be used as an index to indirectly determine the strength of the luminescence. In Figure S7, the PTFE output voltage is twice as high as that of the Kapton regardless of the mixing ratio of the ZnS:Cu to the PDMS, indicating that the luminescence intensity is independent of the mixing ratio, which is confirmed by the experiment (not shown here).

For the woven structure that is shown in Figure 1a, when it is subjected to the stretching force, the two effects of the internal triboelectrification-induced EL from the weft and the external triboelectrification-induced EL from the warp occur simultaneously to enhance the EL. Indeed, each of the tilted conduction and valence bands of the ZnS:Cu, which originate from the potentials due to the triboelectrification processes, are summed up to result in larger bands gradients, as shown in Figure 2g. As a result, the trapped electrons that are due to the sulfur (S) vacancy can easily be detrapped, and in fact, they can freely move into the ZnS conduction band. These electrons can then fall into the Cu impurity state, leading to the emission of light at a wavelength of 510 nm via a radioactive recombination process that is an acceptor type luminescence.[3,16] Nonetheless, the dual triboelectrification (external and internal)-induced electric potential is essentially attributed to the tilting of the band structure inside the ZnS in the woven structures.

For a theoretical understanding of the internal triboelectrification-induced EL mechanism, finite element method simulations were conducted in COMSOL to depict the pores around the ZnS:Cu phosphor inside the PDMS, as shown in Figure 4a. The pore size varies from 2.5 ~ 10 μm. This phenomenon can be explained in terms of the triboelectricification due to the soft frictional contact between the ZnS particles and the PDMS matrix that is due to a pushing force. Since the PDMS is negatively charged relative to the ZnS, it can be assumed that the +q and –q charges are produced in the pores around the gap. The electric potential inside the ZnS:Cu phosphor particle is shown along the diameter with different pore sizes in Figures 4b and 4c. As the pore size is increased, the electric potential of the ZnS is also increased. Figure 4c shows the electric potential that is shown in Figure 4a with different pore sizes; the charge of the q is the same for the simulations. The effect of the pore size on the potential distribution becomes evident, and it is in fact higher for the larger gap between the ZnS:Cu and the PDMS. Therefore,

a bigger pore size can potentially result in larger tilts in the conduction and valence bands as well; that is, a larger gap can enhance the internal triboelectrification-induced EL.

The ZnS is also a known piezoelectric material that produces an external force-induced electric potential.[15,33] But here, during the deformation (compression) from the vertical force, as shown in Figure 4a, the calculated stress is approximately within the range of 0.05 ~ 0.5 MPa, which is considered as insufficient regarding the generation of a piezoelectric potential around the ZnS particles that are embedded in the PDMS; the wurtzite phase of the ZnS is shown in Figure S8. This finding is because it is expected that the piezoelectric d33 coefficient of the ZnS:Cu-PDMS composite structure is of a value that is lower than that of other piezoelectric materials,[17] negating its potential to influence the luminescence process. Thus, it is suggested that the internal EL is associated mainly with the triboelectrification instead of the piezoelectric luminescence.

Figure 5a schematically shows the working process at each step for one cycle where two triboelectrification processes occur, i.e., one during the compression (internal triboelectrification) and the other after the separation (external triboelectrification). Here, the luminescence is associated with the triboelectrification-induced luminescence, which is different from the generally known mechanisms such as electroluminescence, cathodoluminescence,[34,35] and mechanoluminescence in manganese-doped ZnS. Nonetheless, the charge transfer amounts between “ZnS:Cu and PDMS” and “PDMS and PTFE” strongly depend on their relative polarities in terms of the triboelectric series.

When the composite film (ZnS:Cu + PDMS) is pressed by a PTFE force, asymmetric pores are formed between the PDMS and the ZnS:Cu particles. Equal and opposite charges are generated at the gap interfaces in the pores according to the triboelectric properties of the two materials. However, in terms of the PTFE separation, the holes disappear due to the restoration

of the elastic PDMS and the charges are neutralized, thereby changing the internal electric field. Meanwhile, after the contact between the PDMS and the PTFE, their surfaces are oppositely charged, and consequently, an electric field is externally generated around the ZnS:Cu particles; when they come into contact again, the surface charges become neutralized. Nonetheless, the triboelectric charges on the PDMS surface continue to accumulate as the number of frictions/contacts is increased. As a consequence, the electric field also increases, thereby increasing the emission intensity as well. Unlike the PTFE, the triboelectrification of the PDMS with the Kapton shows the opposite character. After the contact, the charges of the Kapton are positive and those of the PDMS are negative, as shown in Figure S9. Nevertheless, the internal triboelectrification process is the same with the PTFE contact.

Figure 5b and 5c show the time evolution of the luminescence intensity for the Kapton and PTFE cases. The luminescence intensity is initially increased, and thereafter it reaches saturation, and it is also strongly dependent on the pushing force. Besides, the luminescence intensity is higher due to the PTFE contact, and also, it is higher than that of the Kapton due to the stronger PTFE triboelectrification. This finding is due to the fact that the maximum luminescence intensity depends on the maximum surface charge.

CONCLUSION

In summary, the possibility of a new self-powered luminescent textile system, with the aim of a light emission that is driven by random body motions without the need for bulky and limited lifetime batteries, has been demonstrated. The ZnS:Cu-based TMEL was fabricated onto the woven fibers of the ZnS:Cu-embedded PDMS composite. The triboelectrification that is due to the contact–separation motion of the friction materials causes a discontinuous electrostatic field. The luminescence can be generated due to the triboelectrification of the ZnS:Cu-

embedded PDMS composite under a mechanical deformation. The tendency of the TI-EL means that it follows the characteristics of a TENG. When the detailed emission measurements were recorded for the contact–separation motion, the TMEL device emitted light from the internal triboelectric field during the contact and from the external triboelectric field during the separation; therefore, the light was emitted twice in one cycle, suggesting that a continuous light can be emitted under various motions. Based on this phenomenon, a self-luminescent textile that successfully demonstrated a triboelectrification-based textile generated luminescence without an external electric power source was designed. This work represents a key step in the pursuit of self-powered wearable display applications. Since the TMEL is based on composite (ZnS:Cu + PDMS) fibers and PTFE fibers, the proposed self-luminescence textile system can be easily fabricated into smart clothes.

METHODS

Fabrication process of the composite material-based luminescent textile. The phosphor particles that were embedded in the soft matrix consist of the GGS 42 ZnS:Cu (Global Tungsten & Powders Corp., United States) and the prepolymer of the Sylgard 184 PDMS (Dow Corning Corp., United States) at a weight ratio of 5:5. After a sufficient mixing, the PDMS cross-linker was added as a curing agent to the mixture of the ZnS:Cu micro size particles in the atmosphere with a weight ratio of 10:1. The mixture was then coated onto a smooth Cu/PET film with a thickness of 300 μm using an automatic bar coater. After a curing in an oven, a large area composite film (20 x 20 cm^2) was detached from the Cu/PET substrate. The characteristics of the green phosphor ZnS:Cu particles are described in previous reports.[3,16] The flat woven-textile fibers were made from the cutting of these composite and PTFE films, both of which are 300-μm -thick, into 3-mm-lengths. The luminescent textile from these fibers was prepared

through the weaving of the warp and the weft. The size of the fabricated textile is 10 x 10 cm^2, and the weave structure is the simplest plain weave.

Fabrication of the TENG. A ZnS:Cu-embedded PDMS composite-based TENG with the dimensions of 2 x 2 cm^2 was realized. A 300-μm-thick composite film that had been deposited on a Cu/PET substrate served as the top friction layer of the generator, while a 150-μm-thick PTFE film that attached on an Al tape electrode served as the opposite friction layer of the generator. The two parts were supported on an acrylic substrate.

Characterization and measurements. The cross-sectional morphology of the ZnS:Cu-embedded composite film was characterized using the JSM-6701F FE-SEM (Jeol Ltd., Japan). The structure of the ZnS:Cu powder was measured using the D8 ADVANCE X-ray diffraction (XRD) device (Bruker Corp., Germany). The ZBT-200 bending tester (Z-tec., South Korea) was utilized to apply the bending strain to the woven textile along the x-axis. The emitted light was measured above the textile using the QE Pro 65000 spectrometer (Ocean Optics Inc., United States). A periodic force was applied to the composite films in an acryl black box with a transparent upper part using a contact−separation friction system to systematically measure the TI-EL emission under different mechanical stresses. The force that was applied to the film was measured using a pressure sensor above a friction material with the dimensions of 1 x 1 cm^2. For the measurement, a spectrometer was used to record the emitted light under the ZnS:Cu-embedded composite film in the acryl box. The friction materials are Kapton, PDMS, and PTFE. The DPO 3052 digital phosphor oscilloscope (Tektronix Inc., United States) was used to detect the open circuit voltage signals that were generated by the TENG.

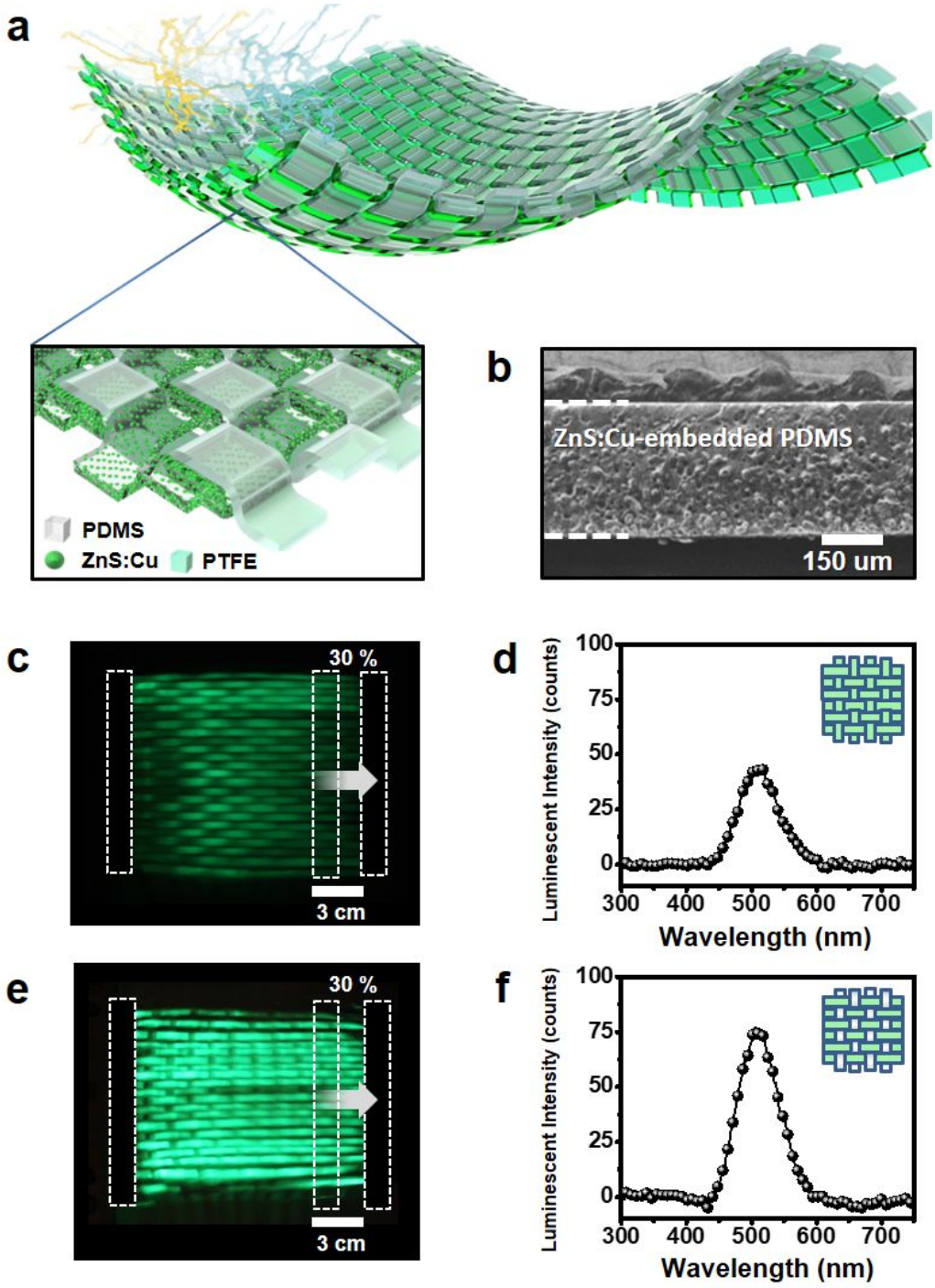

Figure 1. (a) Schematic illustration of the TMEL that was woven using the ZnS:Cu-embedded PDMS composite and the PTFE. (b) Cross-sectional view of the FE-SEM image of a PDMS composite that is ~ 300-um-thick and embedded with ZnS:Cu micro-size particles. Photograph of the luminescent woven textile in the motion along the x-axis with: (c) composite fibers (ZnS:Cu + PDMS), and (e) composite (ZnS:Cu + PDMS) and PTFE fibers. Luminescence

spectra of the textiles woven with: (d) composite fibers (ZnS:Cu + PDMS), and (f) composite (ZnS:Cu + PDMS) and PTFE fibers, respectively. The inset is a schematic image clearly showing the plain woven textile.

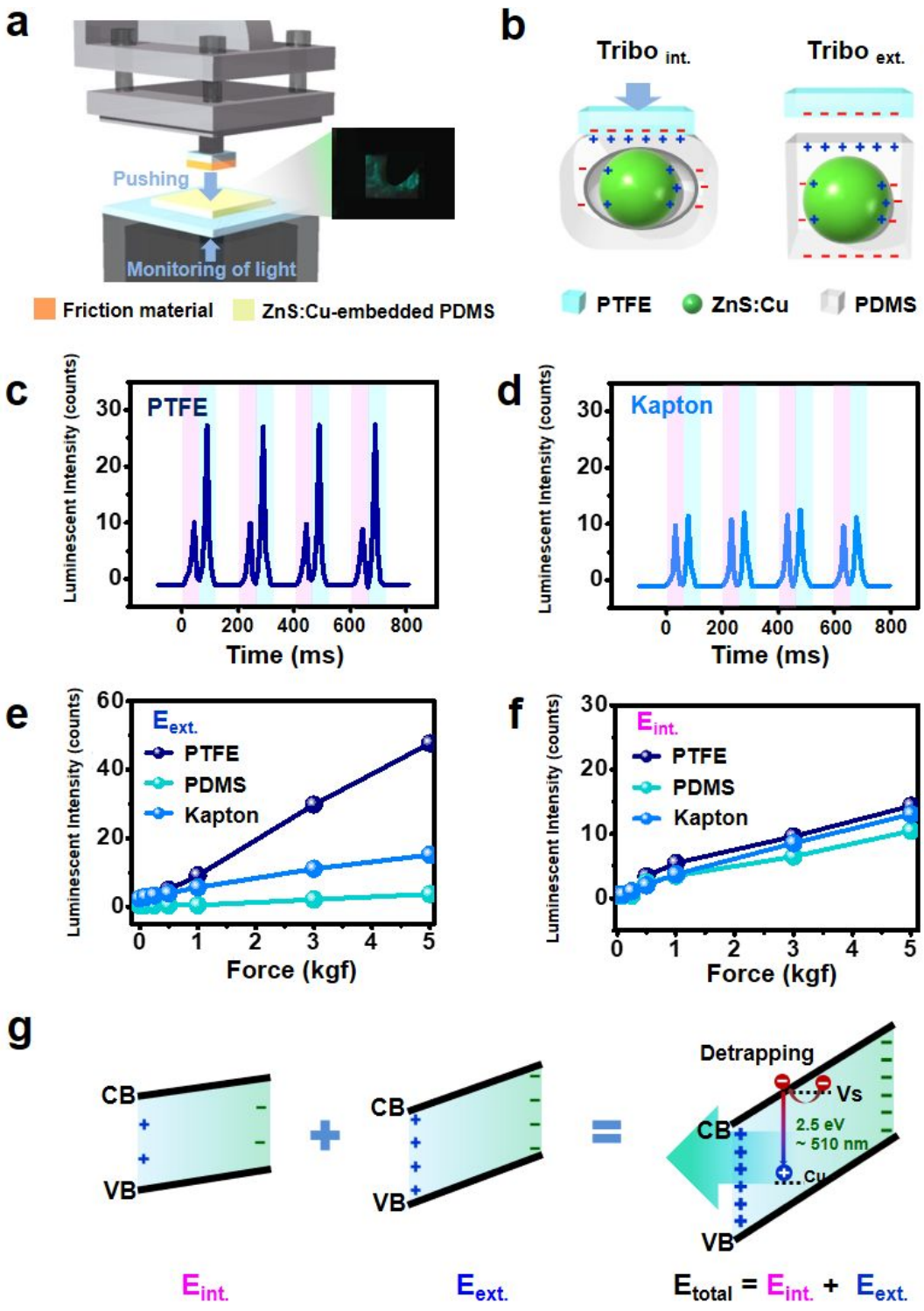

Figure 2. Demonstration of the TI-EL of a composite film. (a) Schematic illustration of the contact–separation approach that was used in this study. The inset is a photograph of the 510 nm emitted ZnS:Cu-embedded PDMS composite film (green color). (b) Schematic diagram of the charge distribution between the materials when the 1 x 1 cm^2 PTFE is used as a friction

material in the pushing state (internal triboelectrification) and for the separation after the pushing state (external triboelectrification), respectively. Luminescent response to the pushing motion (pink color) and the separation motion (sky blue color) using the following friction materials at a pushing pressure of 3 kgf: (c) PTFE, and (d) Kapton. The luminescence spectrum that is induced at various pushing pressures of the friction material due to the: (e) external, and (f) internal triboelectrifications. (g) Band diagram describing the TI-EL mechanism of the ZnS:Cu phosphor.

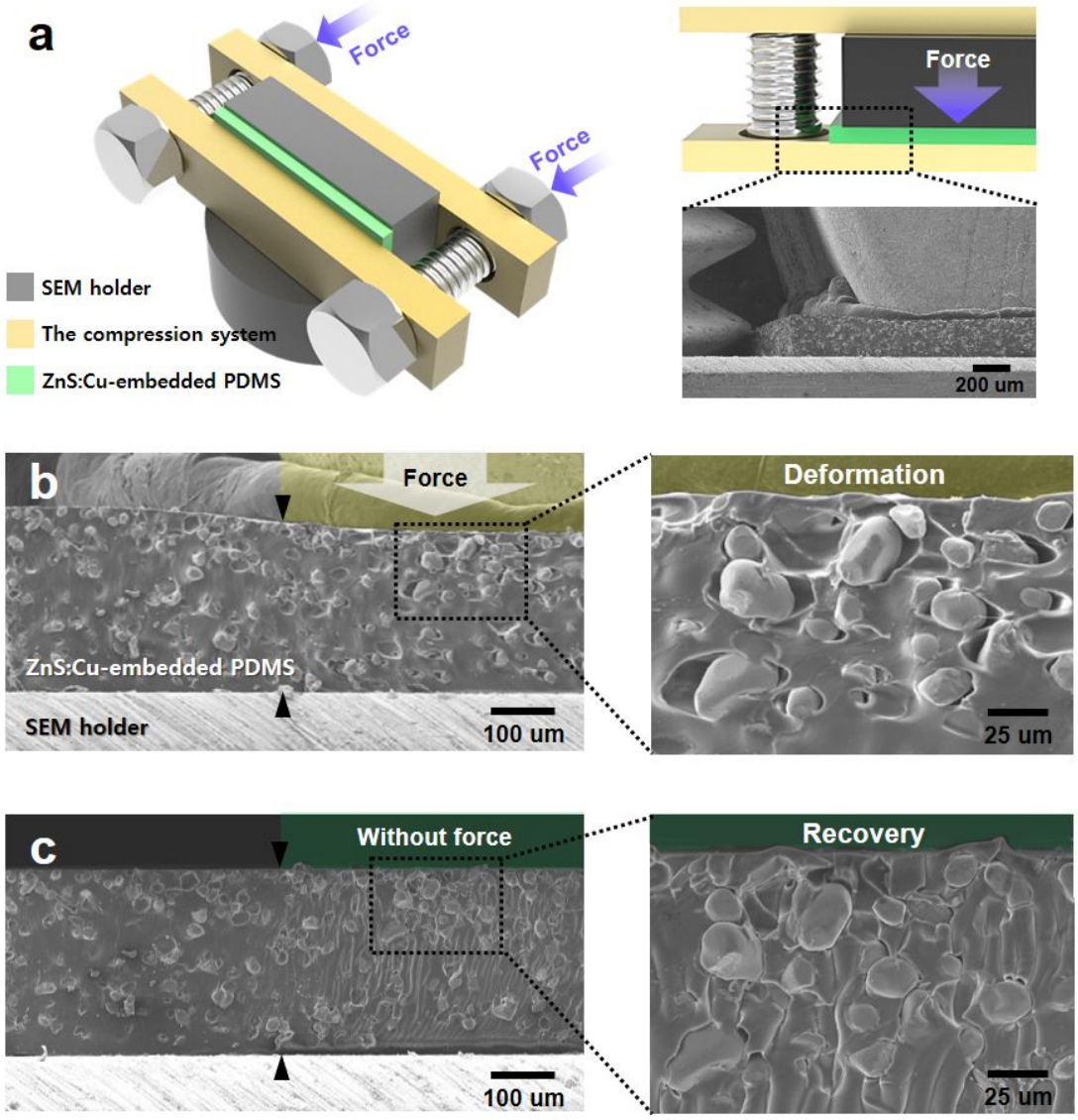

Figure 3. (a) Schematic illustration of a compression system for the monitoring of ZnS:Cu-embedded PDMS composite film with deformation. Inset of the figure shows the cross sectional SEM image of the compressed ZnS:Cu-embedded PDMS composite film. Cross sectional FE-SEM images of the fabricated composite film; (b) with deformation that the pores are formed between the ZnS:Cu and the PDMS by the external force. (c) without deformation by external force that it is recovered again the reduced thickness of the composite film and the formed pores between the ZnS:Cu and the PDMS after the compression system removed.

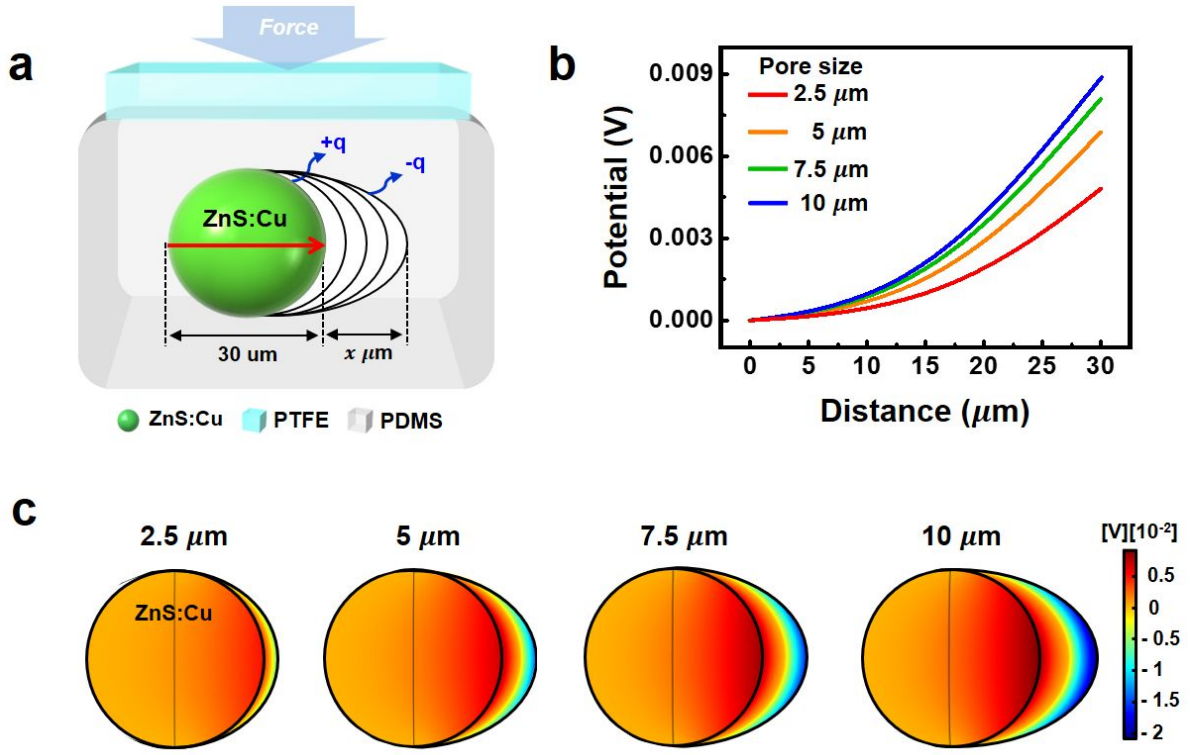

Figure 4. (a) Schematic description of the pores that are formed between the ZnS:Cu and the PDMS by the external force. COMSOL simulation results: (b) numerically calculated output potential distribution, and the (c) surface potential of the ZnS:Cu micro-size particle with different pore gaps.

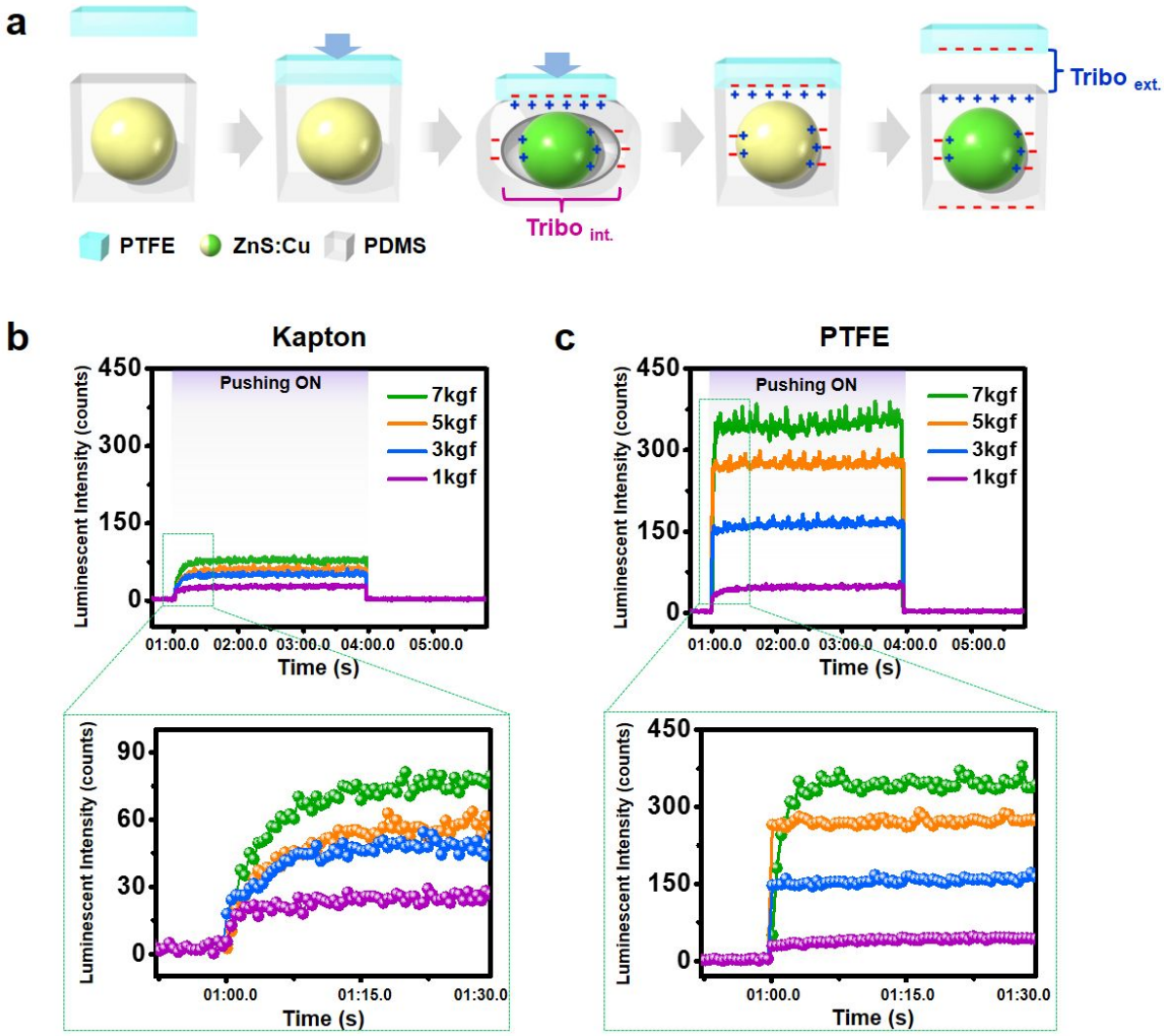

Figure 5. (a) Schematic description of the internal and external triboelectric fields for the ZnS:Cu-embedded PDMS composite and the PTFE in the pushing–separation mode. The luminescence intensity change that is due to the triboelectrification between the composite and (b) the Kapton/ (c) the PTFE at different pushing pressures.

ASSOCIATED CONTENT

Supporting Information

Additional details include the fabrication of a composite film, and the weaving of a luminescence textile; photo images of the plain woven textile-based fibers during stretching; the measurement system for the monitoring of the light emission according to the pushing–separation motion; structural illustration of the motions in which the external and internal triboelectrifications occur; the luminescence spectra of the TI-EL during the pushing–separation motion from the Kapton and the PTFE; cross sectional FE-SEM images of the formed pores naturally in the process of production of composite film without the external force; electrical power output performances of the TENGs for the friction materials and the different mixing ratios of ZnS:Cu in PDMS; XRD of ZnS:Cu powder samples; schematic images regarding the mechanism on the formation of the internal and external triboelectric fields for the composite and the Kapton in the pushing–separation mode.

AUTHOR INFORMATION

Corresponding Authors

*E-mail: kimsw1@skku.edu

Authors Contributions

⊥ H.-J. P and S. M. K. contributed equally to this work

Notes

The authors declare no competing financial interest.

ACKNOWLEDGMENT

This work was financially supported by the Center for Advanced Soft-Electronics as the Global Frontier Project (2013M3A6A5073177) and the Basic Science Research Program (2018R1A2A1A19021947) through the National Research Foundation (NRF) of Korea Grant funded by the Ministry of Science and ICT, and by the "Human Resources Program in Energy Technology (No. 20174030201800)" of the Korea Institute of Energy Technology Evaluation and Planning (KETEP) funded by the Ministry of Trade, Industry & Energy (MOTIE, Korea).

REFERENCES

(1) Eddingsaas, N. C.; Suslick, K. S. Light from Sonication of Crystal Slurries. *Nature*, **2006**, 444, 163

(2) Olawale, D. O.; Dickens, T. W.; Sullivan, G.; Okoli, O. I.; Sobanjo, J. O.; Wang, B. Progress in Triboluminescence-Based Smart Optical Sensor System. *J. Luminesc.,* **2011**, 131, 1407-1418

(3) Jeong, S. M.; Song, S.; Lee, S.-K.; Choi, B. Mechanically Driven Light-Generator with High Durability. *Appl. Phys. Lett.*, **2013**, 102, 051110

(4) Gan, J.; Kang, M. G.; Meeker, M. A.; Khodaparast, G. A.; Bodnar, R. J.; Mahaney, J. E.; Mauryaa, D.; Priya, S. Enhanced Piezoluminescence in Non-Stoichiometric ZnS:Cu Microparticle based Light Emitting Elastomers. *J. Mater. Chem. C*, **2017**, 5, 5387-5394

(5) Greenham, N. C.; Peng, X.; Alivisatos, A. P. Charge Separation and Transport in Conjugated-Polymer-Semiconductor-Nanocrystal Composites Studied by Photoluminescence Quenching and Photoconductivity. *Phys. Rev. B*, **1996**, 54, 17628-17637

(6) de Mello, J. C.; Wittmann, H. F.; Friend, R. H. An Improved Experimental Determination of External Photoluminescence Quantum Efficiency. *Adv. Mater*., **1997**, 9, 230-232

(7) Bredol, M.; Dieckhoff, H. S. Materials for Powder-Based AC-electroluminescence. *Materials*, **2010**, 3, 1353-1374

(8) Bai, G.; Tsang, M.-K.; Hao, J. Tuning the Luminescence of Phosphors: Beyond Conventional Chemical Method. *Adv. Optical Mater.,* **2014**, 3, 431

(9) Han, C. B.; Zhang, C.; Tian, J.; Li, X.; Zhang, L.; Li, Z.; Wang, Z. L. Triboelectrification induced UV Emission from Plasmon Discharge. *Nano Res*., **2015**, 8, 219

(10) Schuster, G. B. Chemiluminescence of Organic Peroxides. Conversion of Ground-state Reactants to Excited-State Products by the Chemically Initiated Electron-Exchange Luminescence Mechanism. *Acc. Chem. Res*., **1979**, 12, 366-373

(11) Miao, W. Electrogenerated Chemiluminescence and Its Biorelated Applications. *Chem. Rev.*, **2008**, 108, 2506-2553

(12) Wang, Z. L. Triboelectric Nanogenerators as New Energy Technology for Self-Powered Systems and as Active Mechanical and Chemical Sensors. *ACS Nano*, **2013**, 7, 9533-9557

(13) Williams, M. W. Triboelectric Charging of Insulating Polymers–Some New Perspectives. *AIP Adv.*, **2012**, 2, 010701

(14) Zhou, Y. S.; Wang, S.; Yang, Y.; Zhu, G.; Niu, S.; Lin, Z.-H.; Liu, Y. Wang, Z. L. Manipulating Nanoscale Contact Electrification by an Applied Electric Field. *Nano Lett.*, **2014**, 14, 1567-1572

(15) Wang, X.; Zhang, H.; Yu, R.; Dong, L.; Peng, D.; Zhang, A.; Zhang, Y.; Liu, H.; Pan, C.; Wang, Z. L. Dynamic Pressure Mapping of Personalized Handwriting by a Flexible Sensor Matrix Based on the Mechanoluminescence Process. *Adv. Mater.*, **2015**, 27, 2324-2331

(16) Wei, X. Y.; Wang, X.; Kuang, S. Y.; Su, L.; Li, H. Y.; Wang, Y.; Pan, C.; Wang, Z. L.; Zhu, G. Dynamic Triboelectrification-Induced Electroluminescence and Its Use in Visualized Sensing. *Adv. Mater.*, **2016**, 28, 6656-6664

(17) Sohn, K.-S.; Timilsina, S.; Singh, S. P.; Choi, T.; Kim, J. S. Mechanically Driven Luminescence in a ZnS:Cu-PDMS Composite. *APL Mater.*, **2016**, 4, 106102

(18) Wang, J.; Yan, C.; Chee, K. J.; Lee, P. S. Highly Stretchable and Self-Deformable Alternating Current Electroluminescent Devices. *Adv. Mater.,* **2015**, 27, 2876-2882

(19) Zhang, Z.; Guo, K.; Li, Y.; Li, X.; Guan, G.; Li, H.; Luo, Y.; Zhao, F.; Zhang, Q.; Wei, B.; Pei, Q.; Peng, H. A Colour-Tunable, Weavable Fibre-Shaped Polymer Light-Emitting Electrochemical Cell. *Nat. Photonics*, **2015,** 9, 233-238

(20) Han, H. Park,; Jeon, E. User Acceptance of a Light-Emitting Diode Vest for Police Officer. *Fashion & Text. Res. J.*, **2013**, 15, 834-840

(21) Stoppa, M.; Chiolerio, A. Wearable Electronics and Smart Textiles: A Critical Review. *Sensors*, 2014, 14, 11957-11992

(22) Castano, L. M.; Flatau, A. B. Smart Fabric Sensors and E-Textile Technologies: A Review. *Smart Mater. Struct.*, **2014**, 23, 053001

(23) Yang, C.-C.; Ngo, T.; Tran, P. Influences of Weaving Architectures on the Impact Resistance of Multi-Layer Fabrics. *Mater. Des.*, **2015**, 85, 282-295

(24) Bijwe, J. Rattan, Influence of Weave of Carbon Fabric in Polyetherimide Composites in Various Wear Situations. *Wear*, **2007**, 263, 984-991

(25) Li, X.; Sun, P.; Fan, L.; Zhu, M.; Wang, K.; Zhong, M.; Wei, J.; Wu, D.; Cheng, Y.; Zhu, H. Multifunctional Graphene Woven Fabrics. *Sci. Rep.*, **2012**, 2, 395

(26) Wen, Z.; Yeh, M.-H.; Guo, H.; Wang, J.; Zi, Y.; Xu, W.; Deng, J.; Zhu, L.; Wang, X.; Hu, C.; Zhu, L.; Sun, X.; Wang, Z. L. Self-Powered Textile for Wearable Electronics by Hybridizing Fiber-Shaped Nanogenerators, Solar Cells, and Supercapacitors. *Sci. Adv.*, **2016**, 2, e1600097

(27) Pu, X.; Li, L.; Song, H.; Du, C.; Zhao, Z.; Jiang, C.; Cao, G.; Hu, W.; Wang, Z. L. A Self-Charging Power Unit by Integration of a Textile Triboelectric Nanogenerator and a Flexible Lithium-Ion Battery for Wearable Electronics. *Adv. Mater.*, **2015**, 27, 2472-2478

(28) Seung, W.; Gupta, M. K.; Lee, K. Y.; Shin, K.-S.; Lee, J.-H.; Kim, T. Y.; Kim, S.; Lin, J.; Kim, J. H.; Kim, S.-W. Nanopatterned Textile-Based Wearable Triboelectric Nanogenerator. *ACS Nano*, **2015**, 9, 3501-3509

(29) Zhong, J.; Zhang, Y.; Zhong, Q.; Hu, Q.; Hu, B.; Wang, Z. L.; Zhou, J. Fiber-Based Generator for Wearable Electronics and Mobile Medication. *ACS Nano*, **2014**, 8, 6273-6280

(30) Jeong, S. M.; Song, S.; Joo, K.-I., Kim, J.; Hwang, S.-H.; Jeong, J.; Kim, H. Bright, Wind-Driven White Mechanoluminescence from Zinc Sulphide Microparticles

Embedded in a Polydimethylsiloxane Elastomer. *Energy Environ. Sci.*, **2014**, 7, 3338-3346

(31) Zhong, J.; Zhong, Q.; Chen, G.; Hu, B.; Zhao, S.; Li, X.; Wu, N.; Li, W.; Yua, H.; Zhou, J. Surface Charge Self-Recovering Electret Film for Wearable Energy Conversion in a Harsh Environment. *Energy Environ. Sci.*, **2016,** 9, 3085-3091

(32) Ko, Y. H.; Nagaraju, G.; Lee, S. H.; Yu, J. S. PDMS-Based Triboelectric and Transparent Nanogenerators with ZnO Nanorod Arrays. *ACS Appl. Mater. Interfaces*, **2014**, 6, 6631-6637

(33) Fang, H.; Wang, X.; Li, Q.; Peng, D.; Yan, Q.; Pan, C. A Stretchable Nanogenerator with Electric/Light Dual-Mode Energy Conversion. *Adv. Energy Mater.*, **2016**, 6, 1600829

(34) Wu, X. L.; Siu, G. G.; Fu, C. L.; Ong, H. C. Photoluminescence and Cathodoluminescence Studies of Stoichiometric and Oxygen-Deficient ZnO Films. *Appl. Phys. Lett.*, **2001**, 78, 2285-2287

(35) Bylander, E. G. Surface Effects on the Low-Energy Cathodoluminescence of Zinc Oxide. *J. Appl. Phys.*, **1978**, 49, 1188

Table of Contents

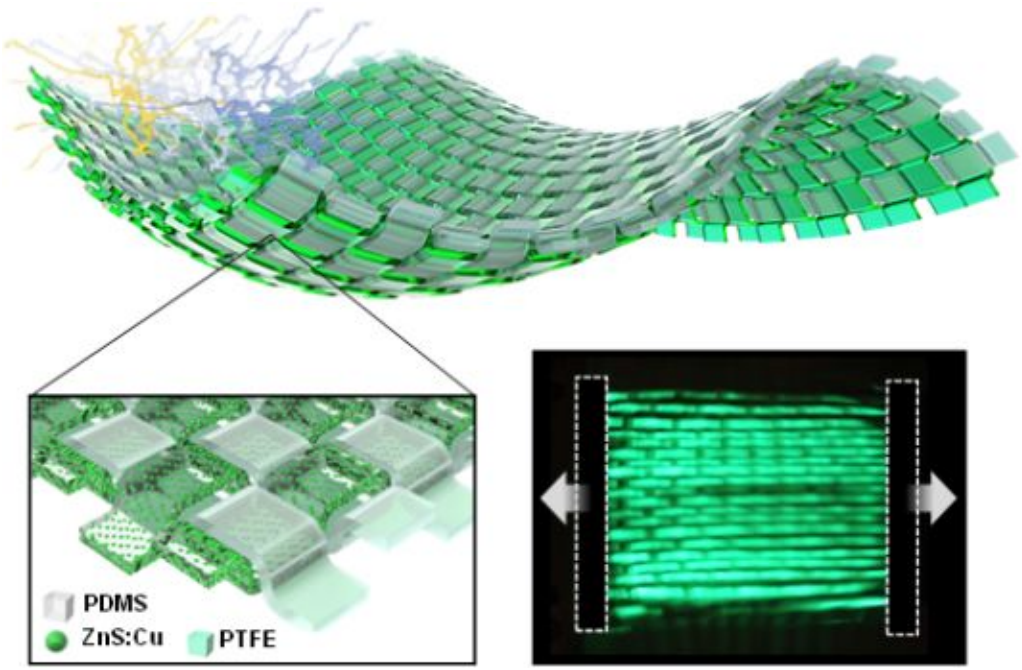
PDMS
ZnS:Cu
PTFE